BRCORP
TECHNOLOGY | INNOVATION | INDUSTRY

International Journal of
Advanced Structures and Geotechnical Engineering
ISSN 2319-5347, Vol. 05, No. 01, January 2016

Modeling the Behavior of Granular Materials under Plane Strain Compression by 3D DEM

MD. MAHMUD SAZZAD*1, RIPON KUMER SHAHA2, MD. SHEHABUL ISLAM3
[1]*Department of Civil Engineering, Rajshahi University of Engineering & Technology, Bangladesh*
[2]*Department of Civil Engineering, Lakshmipur Polytechnic Institute, Lakshmipur, Bangladesh*
[3]*Kwun Tong Apparels Ltd., Adamjee Export Processing Zone, Bangladesh*
Email:mmsruet@gmail.com, riponce07@gmail.com, shihab_ce@yahoo.com

Abstract: The in-situ stress condition in dam or embankment of roads corresponds well to the plane strain condition. In this study, simulation of plane strain compression (PSC) test was numerically performed to explore the behavior of granular materials such as sand at macro- and micro-scale using the discrete element method (DEM). Three cubical shaped samples having different void ratios were numerically prepared using eleven different sizes of spheres whose diameters range from 3 to 4 mm. The spheres were randomly placed in a cubical shaped sample in such a way that, at the initial stage, no sphere can touch the other and later, the sample was compressed isotropically to 100 kPa at different stages using the periodic boundary. The isotropically compressed samples were used for numerical experiment under PSC. It is noted that the numerical results are consistent to that observed in the experiments under PSC for different void ratios. Evolution of dilatancy index is observed and found to be dependent on the void ratio of the samples, in particular at the small strain level, for PSC. However, it is observed that the dilatancy index curves approach a unique state at large strain. The normalized work (normalized by the mean stress) exhibits almost unique behavior, particularly at small strain level, regardless of the void ratio. The evolution of the ratio of strong contacts to total number of stable contacts (a stable contact is a contact that have met a certain stability requirement, i.e., each particle has at least three contacts) with axial strain is also monitored and it is noted that the ratio is not a function of initial void ratios of the samples. The number of strong contacts, on an average, is the 30% of the total stable contacts in an assembly of granular system during shear regardless of the void ratios of samples.

***Keywords**: Plane strain compression, Dilatancy index, Micro parameters, Discrete element method.*

1. Introduction:

Granular materials exhibit intricate behavior under different stress conditions such as triaxial stress condition, plane strain condition, etc. Plane strain condition is often observed in natural state such as the long embankments for roads or railways where the strain parallel to the longitudinal axis of the embankment is almost zero. So, the investigation of the macro- and micro-behaviors of granular materials for PSC is significant. The macro- and micro-mechanical characteristics of granular assembly are strongly dependent on the properties of the constituent individual particles. The mechanical responses of granular material are different due to the variation of stress paths that have already been reported by several experimental studies. For example, Cornforth (1964) reported that the internal friction angle is more than 4° greater for plane strain condition than triaxial condition in dense state. The initiation of shear band is also affected by the difference in the stress paths. For example, Peters et al. (1988) reported that shear band initiation is easier under plane strain condition than axis symmetric condition. In the experimental studies, the macro mechanical responses such as stress, strain, volumetric strain, dilatancy index, etc. can be observed easily. On the other hand, it is difficult to investigate the knowledge of micro behaviors of granular materials in PSC test under different samples. Therefore, the knowledge of the micro characteristics is important to develop physically sound and micro-mechanical based constitutive models. This inherent limitation of experiments can be evaded using the numerical methods such as DEM (Cundall and Strack, 1979), which can model the discrete behavior of granular materials and provide inside into the micro features of the particulate system. Using DEM, the evolution of micro variables can be studied and micro data can be extracted at any stage of simulation. However, there are inadequate studies found in the literature that considered PSC in 3D DEM. For example, Ng (2004) considered several stress paths with different sample preparation methods to report the macro and micro responses including PSC by 3D DEM. Sazzad and Suzuki (2012) presented a comparative study of the macro- and micro-mechanical behavior by considering the conventional triaxial and plane strain compression tests. Sazzad et al. (2015) presented the micro-features of granular materials under PSC conditions. Even though several studies are conducted by DEM, a comprehensive study of the evolution of the macro- and micro-parameters under PSC are still lacking. This study presents a comprehensive study of the different macro- and micro-mechanical behaviors of granular materials under PSC by 3D DEM. For this purpose, three isotropically compressed samples of different void ratios are considered to simulate the plane strain behavior. Isotropically compressed samples are sheared at PSC and the macro- and micro-scale data are recorded at equal interval of time steps. The data are presented to explore the macro- and micro-characteristics of granular materials under PSC.

2. DEM Features:

Discrete element method (DEM) is one of the most popular discrete approaches that describe the internal behaviors of granular materials such as sand in particulate system. The method was first introduced by Cundall (1971) for rock mass problem and later, extended to soil (Cundall and Strack, 1979). DEM has been proved to be a useful tool to understand the physical process such as rotation, acceleration, contact force, etc. of a particle during shear. DEM has been used successfully in different disciples of science and engineering. The advantage of DEM is that the micro data can be monitored and extracted at any stage of the simulation for further analysis. The fundamental idea of DEM is that each particle is modeled as an element which can make and break contact with the neighbor elements included in the model. The DEM uses an explicit time finite-difference scheme in which the calculation cycle includes the application of Newton's second law of motion and a force displacement law. The particle accelerations are calculated using the following equations:

$$m\ddot{x}_i = \sum F_i \qquad i = 1-3 \qquad (1)$$

$$I\ddot{\theta} = \sum M \qquad (2)$$

where, F_i are the force components on each particle; M is the moment; m is the mass; I is the moment of inertia; x_i are the components of translational acceleration and $\ddot{\theta}$ is the rotational acceleration of the particle.

3. About OVAL:

OVAL (Kuhn, 2006) is a computer program used to simulate the discrete behavior of granular materials in this study. The effectiveness of OVAL has already been recognized (Kuhn, 1999; Kuhn, 2005; Sazzad and Suzuki, 2013, Sazzad, 2014). In OVAL, a simple contact force mechanism is included in the system consisting of linear spring both in normal and tangential directions and a frictional slider. The coefficients of viscosity for translational and rotational body damping are used in this program that represent a fraction of the critical damping $2\sqrt{mk_n}$ and $2r\sqrt{Ik_t}$, where r, k_n and k_t denote the radius, normal and tangential contact stiffness of the particle, respectively.

4. Sample Preparation Method:

In the present study, the sample preparation consists of two phases. One is sample generation and the other is sample consolidation. In the sample generation phase, a total of 8000 spheres having diameters ranging from 3 to 4 mm consisting of 11 different sizes were generated. The spheres were randomly placed with equally spaced grids of a cubical frame. The sample at this phase was very sparse. In the sample consolidation phase, the initial sparse sample was consolidated by assigning interparticle friction coefficient of 0, 0.2 and 0.4 for the first, second and third samples. Then, the cubical shaped sample was compressed isotropically to 100 kPa using the periodic boundaries. However, the desired interparticle friction coefficient (i.e., 0.5) was used during shear. The void ratios of three isotropically compressed samples after the end of the consolidation are 0.58, 0.68 and 0.73, respectively while the average coordination number of three isotropically compressed samples after the end of the consolidation are 5.9, 4.8 and 4.2, respectively. The average coordination number is defined by the equation (3).

5. Simulation of PSC Tests:

Simulation of PSC test was carried out by applying a very small strain increment of 0.00002% vertically downward in x_1-direction and keeping the strain in x_2-direction zero (i.e. $d\varepsilon_2 = 0$) while keeping the stress in x_3-direction constant (100 kPa). The simulation condition of PSC test with the reference axes is shown in Figure 1. The DEM parameters used in the study for shear are shown in Table 1.

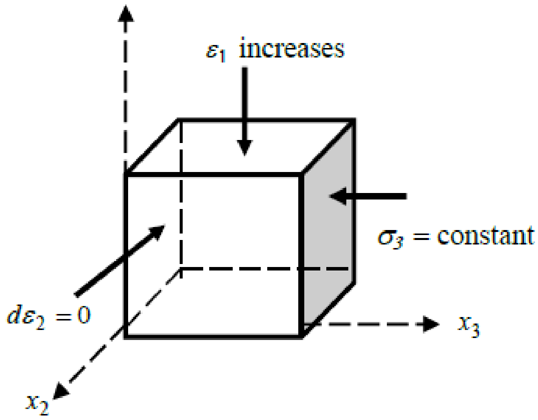

Figure 1: Simulation conditions used in the present study with reference axes

Table 1: DEM parameters used in the study

DEM parameters	Value
Normal contact stiffness (N/m)	1×10^6
Tangential contact stiffness (N/m)	1×10^6
Mass density (Kg/m^3)	2600
Increment of time step (s)	1×10^{-6}
Interparticle friction coefficient	0.50
Coefficient of viscosity for translational and rotational body damping	0.05

6. Macro-mechanical Results:

The simulated stress-strain behavior for plane strain condition under different void ratios is depicted in Figure 2. Note that the stress ratio, σ_1/σ_3, for the densest sample (void ratio 0.58) attains a peak at small strain level followed by huge strain softening whereas for loosest sample (void ratio 0.73), σ_1/σ_3 gradually increases with axial strain ε_1, where σ_1 and σ_3 are the stresses in x_1- and x_3-direction, respectively. Note also that the stress ratio σ_1/σ_3 merge each other at an axial strain of 10%, regardless of the void ratio of the samples. This numerical result is consistent with the experiments under plane strain condition (e.g., Cornforth, 1964). Similar tendency is also noticed in Figure 3 for the relationship between the stress ratio σ_2/σ_3 and ε_1, where σ_2 is the stress in x_2-direction. However, the value of σ_2/σ_3 is lesser compared to σ_1/σ_3 at the same strain level.

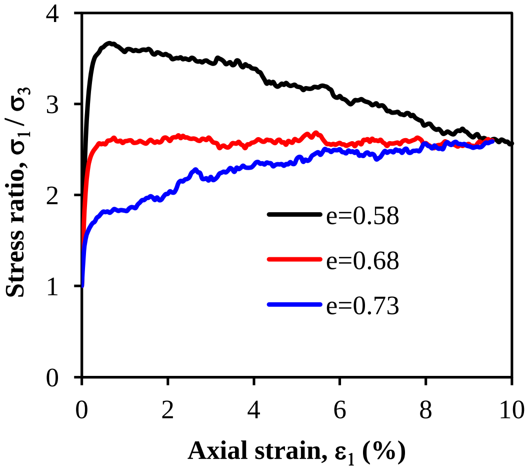

Figure 2: Relationship between stress ratio σ_1/σ_3 and axial strain ε_1

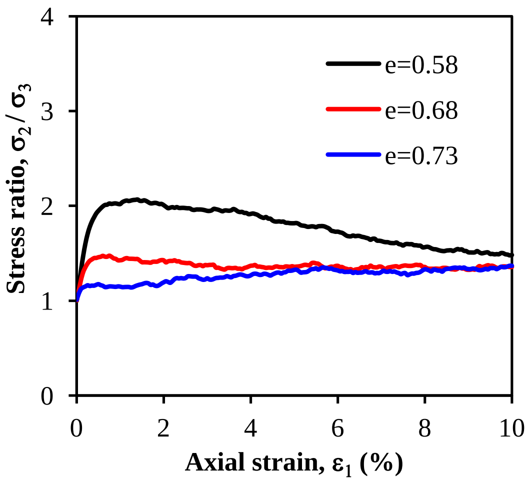

Figure 3: Relationship between stress ratio σ_2/σ_3 and axial strain ε_1

Figure 4, depicts the relationship between the volumetric strain ε_v and axial strain ε_1. The volumetric strain is defined here as $\varepsilon_v = \varepsilon_1 + \varepsilon_2 + \varepsilon_3$, where ε_1, ε_2 and ε_3 are the strains in x_1-, x_2- and x_3-direction, respectively. A positive value ε_v in Figure 4 represents compression while a negative value of ε_v represents dilation. Note that the volumetric strain depicts huge dilation in case of the densest sample (void ratio 0.58) whereas the loosest sample (void ratio 0.73) depicts compression. Similar tendency is noticed in experiments under PSC.

The evolution of the dilatancy index with ε_1 is depicted in Figure 5. The dilatancy index is defined here as $-d\varepsilon_v/d\varepsilon_1$, where $d\varepsilon_v$ is the change of volumetric strain and $d\varepsilon_1$ is the change of axial strain.

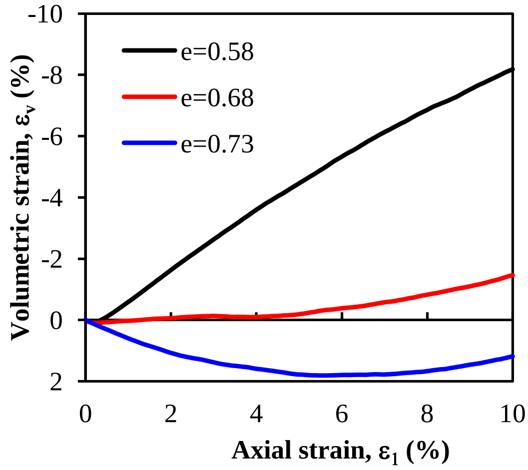

Figure 4: Relationship between volumetric strain ε_v and axial strain ε_1

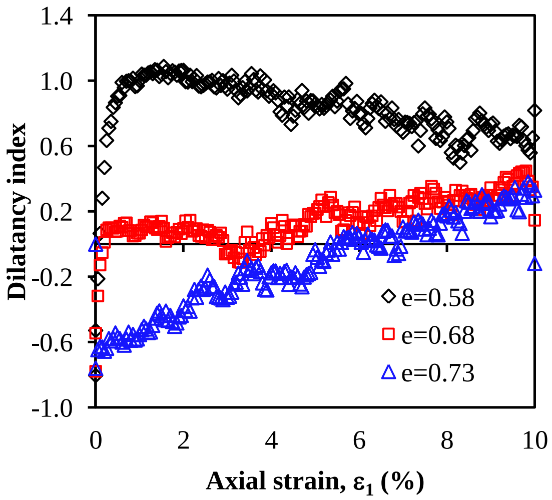

Figure 5: Evolution of dilatancy index with axial strain ε_1

Note that the evolution of dilatancy index is dependent on the void ratio of the sample. For sample having void ratio of 0.58, the dilatancy index reaches its peak at a small strain level. The dilatancy index is negative at the very small strain level regardless of the void ratio indicating the compression governing behavior at the initial stage of simulation. However, it is depicted in Figure 5 that the dilatancy index approaches a unique state at large strain.

The normalized work done for different samples having different void ratios is depicted in Figure 6. The work done by the boundary stresses per unit of the original volume of sample is calculated. It is calculated from the work rate $\frac{V_c}{V_i}\int \sigma_{ij}\dot{F}_{ik}F_{kj}dt$ (Kuhn, 2006), where V_c is the current volume, V_i is the initial volume and σ_{ij} is the Cauchy stress and is cumulative from the beginning of the simulation. The total work done is normalized by the mean stress $p=(\sigma_1+\sigma_2+\sigma_3)/3$. Note that the normalized work depicts a unique behavior at small strain level.

7. Micro-mechanical Responses:

Figure 7 depicts the evolution of average coordination number and slip coordination number with ε_1 in PSC tests for samples having different void ratios. The coordination number and slip coordination number is defined as follows (Sazzad, 2014):

$$Z=\frac{2\times N_c}{N_p} \quad (3)$$

$$Z_{sl}=\frac{2\times N_s}{N_p} \quad (4)$$

Here, N_c is the total number of contact between particles, N_s is the total number of slip contact between particles and N_p is the total number of particles used in the simulation. Note that average coordination number decreases significantly at the beginning of the shear for sample having void ratio of 0.58, which is due to the rearrangement of fabric at the beginning of shear. By contrast, contact disintegration is comparatively lower for sample having void ratio of 0.68 and very few for sample having void ratio of 0.73. Note, however, that the average coordination number merges each other at an axial strain of 2% indicating almost same number of contact formation and contact disintegration after that state of strain, even though the void ratios are different.

The slip coordination number, on the other hand, depicts a different tendency at the beginning of the simulation. For dense sample (void ratio 0.58), the slip coordination number increases almost up to the peak state (Figure 2) and then starts decreasing. However, the slip coordination number merges each other at an axial strain of 2%, which is similar to the average coordination number.

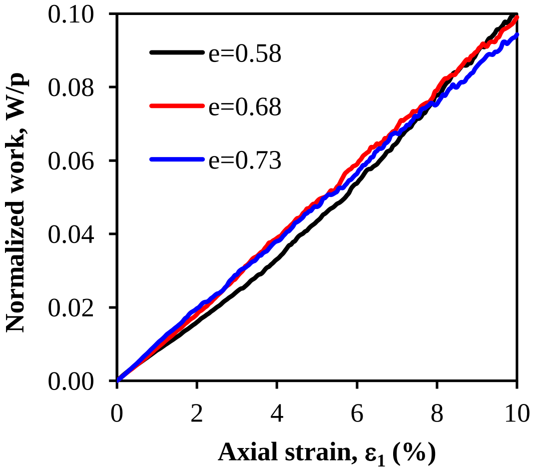

Figure 6: Evolution of normalized work with axial strain ε_1

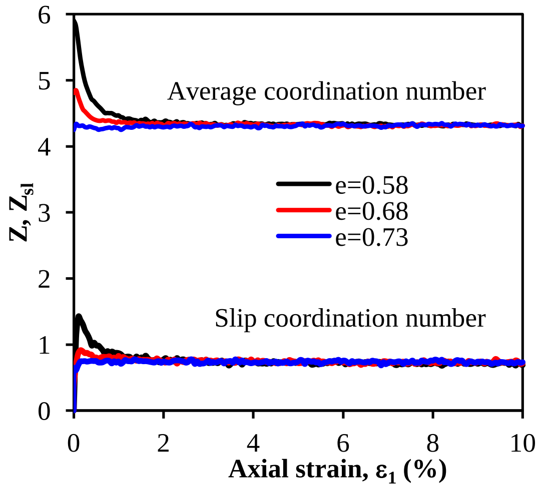

Figure 7: Evolution of average and slip coordination number with axial strain ε_1

The ratio of strong contacts to the total stable contacts is depicted in Figure 8. It is represented as follows:

$$R=\frac{N_c^s}{N_{stb}} \quad (5)$$

where N_c^s is the number of strong contacts, N_{stb} is the total number of stable contacts (a stable contact is a contact that have met a certain stability requirement, i.e., each particle has at least three contacts) and R is the ratio of strong contacts to the total stable contacts. A contact is said to be a strong contact if it carries contact force greater than the average contact force. Average contact force is defined as follows (Kuhn, 2006):

$$f_{ave}=\sqrt{\sum_{k=1}^{N_c}\left|f^k\right|^2 \Big/ N_c} \quad (6)$$

where f^k is the $k-$th contact force. R decreases with ε_1 at the beginning of the simulation and remains almost constant with ε_1. Interesting to note that the evolution of R with ε_1 is similar and almost unique regardless of the void ratio of the sample. This indicates that the ratio of strong to total contacts is not a function of initial void ratio of the samples. It should also be noted that the number of strong contacts, on an average, is the 30% of the total contacts in an assembly of granular system.

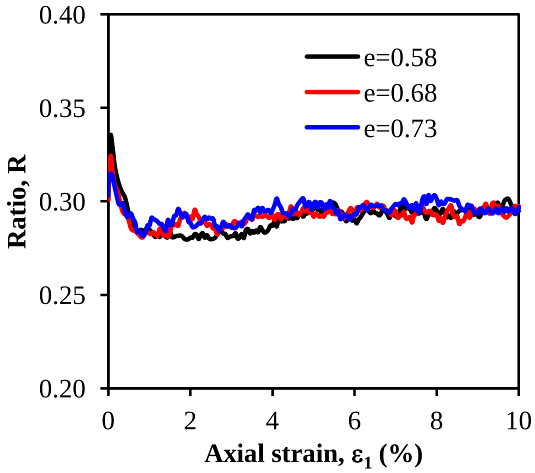

Figure 8: Evolution of R with ε_1 for samples of different initial void ratios under PSC

7. Conclusions:

In this study, a numerical simulation is carried out for three different samples of different void ratios under PSC test to investigate the behaviors of granular materials at micro- and macro-scale. Three cubical shaped numerical samples were prepared in different stages using a total of 8000 spheres to conduct PSC test. The simulated behaviors are compared with the experiments to warrant the validity of the present simulations. It is observed that the simulated macro results are consistent to that usually observed in experiments under PSC. It demonstrates the versatility of the present simulation considering DEM, a numerical tool that allows the monitoring of the micro-scale behaviors in addition to the macro-scale behavior. Some of the findings of this study can be summarized as follows:

i) The evolution of the dilatancy index is dependent on the void ratio of the sample. However, it is observed that the dilatancy index curves approach a unique state at large strain.

ii) The normalized work exhibits almost unique behavior, particularly at small strain level, regardless of the void ratio.

iii) Evolution of average and slip coordination numbers is independent of the void ratio of the sample for PSC at the larger strain.

iv) The ratio of strong contacts to total stable contacts is not a function of initial void ratios of the samples.

v) The number of strong contacts, on an average, is the 30% of the total stable contacts in an assembly of granular system during shear, regardless of the void ratio.

References:

[1] Cornforth, D. H. (1964). "Some experiments on the influence of strain conditions on the strength of sand.", *Geotechnique*, 14(2), 143–167.

[2] Cundall, P. A. (1971). "A computer model for simulating progressive, large scale movements in blocky rock systems.", In: Proceedings of the ISRM Symposium on Rock Fracture, Nancy,France, A. A. Balkama, Rotterdam, Paper II-8, pp. 129–136.

[3] Cundall, P. A., and Strack, O. D. L.(1979).**"**A discrete numerical model for granular assemblies.**"**, *Geotechnique*, 29(1), 47-65.

[4] Kuhn, M. R. (1999). **"** Structured deformation in granular materials.***"**, Mechanics of Materials,* 31(6), 407-429.

[5] Kuhn, M. R. (2005). **"**Are granular materials simple? An experimental study of strain gradient effects and localization**"**, *Mechanics of Materials*, 37(5), 607-627.

[6] Kuhn, M. R. (2006). **"**OVAL and OVALPLOT: Programs for analyzing dense particle assemblies with the discrete element method.**"**, http://faculty.up.edu/kuhn/oval/doc/oval_0618.pdf., last access: April 10,2012.

[7] Ng, T. -T.(2004)." Macro-and micro-behaviors of granular materials under different sample preparation methods and stress paths.", *International Journal of Solids and Structures*, 41(21), 5871-5884.

[8] Peters, J. F., Lade, P. V., and Bro, A. (1988). "Shear Band Formation in Triaxial and Plane Strain Tests", *Advanced Triaxial Testing of Soil and Rock*, ASTM STP977; Robert T. Donaghe, Ronald C., Chancy and Marshall L. Silver Eds., Philadelphia, 604-627.

[9] Sazzad, K., and Suzuki, K. (2012). "A comparison between conventional triaxial and plane-strain compression on a particulate system using 3D DEM.", *Acta Geotechnica Slovenica*, 9(2), 17-23.

[10] Sazzad, M. M. (2014). "Micro-scale behavior of granular materials during cyclic loading.", *Particuology*, Vol. 16, 132–141.

[11] Sazzad, M. M. and Suzuki, K. (2013). "Density dependent macro-micro behavior of granular materials in general triaxial loading for varying intermediate principal stress using DEM.", *Granular Matter*, 15(5), 583-593.

[12] Sazzad, M. M., Shaha, R. K., Islam, M. S. and Kawsari, S. (2015). 'Macro and Micro Responses of Granular Materials under Plane Strain Compression by 3D DEM.", *International Journal of Advances in Structural and Geotechnical Engineering*, 4(2), 114-119.